BASIC RESEARCH www.jasn.org

Disruption of Myosin 1e Promotes Podocyte Injury

Mira Krendel,* Sangwon V. Kim,† Tim Willinger,† Tong Wang,‡ Michael Kashgarian,§ Richard A. Flavell,†‖ and Mark S. Mooseker*§¶

*Department of Molecular, Cellular and Developmental Biology, Yale University, New Haven, Connecticut, and Departments of †Immunobiology, ‡Cellular and Molecular Physiology, §Pathology, and ¶Cell Biology, School of Medicine, Yale University, New Haven, Connecticut; and ‖Howard Hughes Medical Institute, Chevy Chase, Maryland

ABSTRACT

Myosin 1e (Myo1e) is one of two Src homology 3 domain–containing "long-tailed" type I myosins in vertebrates, whose functions in health and disease are incompletely understood. Here, we demonstrate that Myo1e localizes to podocytes in the kidney. We generated Myo1e-knockout mice and found that they exhibit proteinuria, signs of chronic renal injury, and kidney inflammation. At the ultrastructural level, renal tissue from Myo1e-null mice demonstrates changes characteristic of glomerular disease, including a thickened and disorganized glomerular basement membrane and flattened podocyte foot processes. These observations suggest that Myo1e plays an important role in podocyte function and normal glomerular filtration.

J Am Soc Nephrol 20: 86–94, 2009. doi: 10.1681/ASN.2007111172

Myosins are molecular motors that translocate cargo along actin filaments in an ATP-dependent manner. Members of the myosin superfamily, which includes at least 24 myosin classes,[1] contribute to a variety of intracellular functions, including organelle transport, actin reorganization, and cell signaling. Genetic evidence in mice and humans links myosin mutations to hearing and vision defects, neurologic problems, cardiomyopathies, immune system disorders, pigmentation defects, and cancer.[2]

This study focuses on physiologic roles of myosin 1e (myo1e), a class I myosin. Class I myosins consist of a single motor domain, a neck domain that binds one or more calmodulin (or calmodulin-like) light chains, and a cargo-binding tail domain.[2] Some class I myosins have tails that consist of a single domain, termed tail homology 1 (TH1) domain. This domain is basic in charge and may effect interactions with negatively charged phospholipids. Other class I myosins, including myo1e, have longer tails that in addition to TH1 include a proline-rich TH2 domain and C-terminal Src homology 3 domains. Humans and mice express eight myosin I isoforms (1a through h); functions of three myosin I isoforms (1a, 1c, and 1f) have been previously analyzed using genetic manipulation in mice.[3] Mice lacking myo1a, a myosin that is expressed exclusively in intestinal epithelial cells, exhibit defects in the organization of the intestinal brush border.[4] Myo1c has been implicated in the adaptation by the inner ear sensory hair cells; the importance of myo1c for adaptation has been established, in part, using transgenic mice expressing a mutant version of myo1c that could be selectively inhibited using a modified ADP analog.[5] Knockout (KO) of myo1f, a long-tailed Myo1 closely related

Received November 6, 2007. Accepted August 28, 2008.

Published online ahead of print. Publication date available at www.jasn.org.

M. Krendel and S.V.K. contributed equally to this work.

M.K.'s current affiliation is Department of Cell and Developmental Biology, SUNY Upstate Medical University, Syracuse, New York. S.V.K.'s current affiliation is Helen L. and Martin S. Kimmel Center for Biology and Medicine at the Skirball Institute of Biomolecular Medicine, NYU School of Medicine, New York, New York.

Correspondence: Dr. Mira Krendel, Department Cell and Developmental Biology, SUNY Upstate Medical University, 750 East Adams Street, Syracuse, NY 13210. Phone: 315-464-8527; Fax: 315-464-8535; E-mail krendelm@upstate.edu

to myo1e, results in defects in neutrophil migration, which are linked to changes in integrin exocytosis and enhanced cell-substrate adhesion.[6]

Myo1e is expressed in a wide variety of tissues, including spleen, kidney, small intestine, pancreas, brain, and the immune system.[6,7] We previously determined that myo1e tail binds endocytic proteins dynamin and synaptojanin and found that inhibition of myo1e functions in cultured fibroblasts led to defects in endocytosis.[8] To analyze myo1e functions *in vivo*, we developed a myo1e-KO mouse and characterized its phenotype. Myo1e was expressed in the glomerular visceral epithelial cells, or podocytes, which play a central role in glomerular filtration. Myo1e-null mice exhibited defects in glomerular filtration and organization, which were similar to glomerular defects observed in inherited renal diseases that have been linked to mutations in podocyte-expressed proteins in humans.[9,10] Thus, myo1e seems to be necessary for normal renal filtration and disruption of myo1e functions may contribute to renal disease.

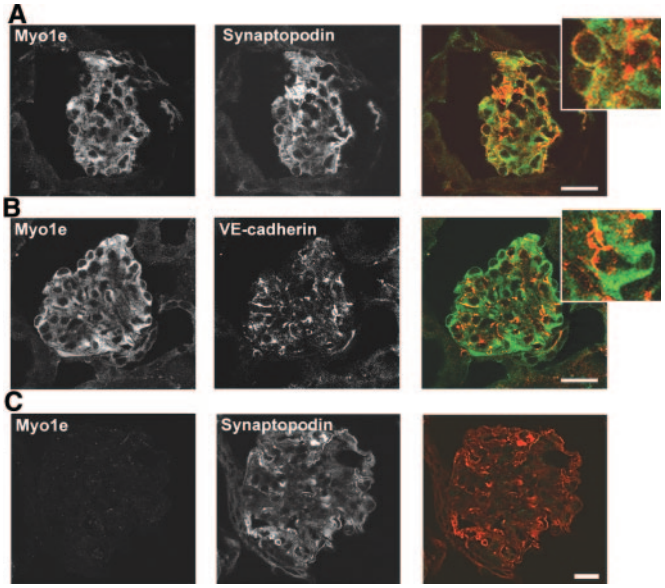

Figure 1. Myo1e localization in mouse kidney. (A through C) Frozen kidney sections prepared from WT mice (A and B) and Myo1e-KO mice (C) were double labeled with antibodies against myo1e and either podocyte marker synaptopodin or endothelial cell marker VE-cadherin. Myo1e co-localized with synaptopodin (A) but not with VE-cadherin (B). No labeling with Myo1e antibodies was observed in the KO mice (C). Merged images show Myo1e in green and synaptopodin or VE-cadherin in red. Insets in A and B show enlargements of selected regions of the merged images. Bar = 20 μm.

RESULTS

Myo1e Is Expressed in Renal Podocytes

Staining of mouse kidney sections with antibodies against myo1e revealed that in the kidney, myo1e was predominantly expressed in the glomeruli (Figure 1). Myo1e partially co-localized with podocyte-specific marker synaptopodin in podocyte foot processes (Figure 1A). In addition to foot process labeling, myo1e exhibited prominent cytoplasmic staining. Endothelial marker VE-cadherin was located in close proximity to myo1e but did not overlap with myo1e (Figure 1B), indicating that myo1e is expressed in podocytes rather than in glomerular endothelial cells.

Immunoblotting and immunofluorescence labeling of cultured mouse podocytes with antibodies against myo1e confirmed that it was expressed in podocytes (Figure 2). Myo1e was localized to punctate structures, some of which were also labeled with anti-synaptopodin antibodies (Figure 2B). In some cells, myo1e was enriched in the areas of cell–cell contacts, where it co-localized with cell adhesion protein β-catenin (Figure 2C). The observed staining pattern was specific for myo1e because labeling with nonimmune IgG showed no enrichment in cell–cell junctions or cytoplasmic punctae (Figure 2D), and labeling with antibodies against nonmuscle myosin IIA (myo2a) revealed a different pattern of localization, with myo2a being localized along actin stress fibers (Figure 2E).

Generation of Myo1e-KO Mice

To generate Myo1e-KO mice, we introduced loxP-recombination sites into Myo1e gene by homologous recombination in embryonic stem cells. Cre-mediated recombination in germline cells was then used to remove loxP-flanked exon 4 from the mouse Myo1e genomic sequence (Figure 3A and Supplemental Methods). In the mutant Myo1e allele, only the first 80 codons are expected to be translated, followed by a stop codon. The KO approach was designed with the goal of achieving a constitutive disruption of myo1e protein expression in all tissues. Mice were genotyped using genomic PCR, and the absence of myo1e protein was confirmed by Western blotting and immunofluorescence staining (Figures 1C and 3).

Myo1e-KO Mice Have Kidney Disease

Myo1e-KO mice did not exhibit any visible abnormalities at birth, their growth rates and lifespan did not differ from those of wild-type (WT) mice, and no obvious defects were detected in any of their internal organs other than kidneys. Analysis of urine samples collected from myo1e-null mice showed high levels of proteinuria (Figure 4), as well as the presence of leukocytes and hemoglobin in the urine of KO mice. Possible causes of proteinuria include disruption of the glomerular filtration barrier or abnormalities in protein reabsorption in the renal proximal tubules. Under normal conditions, proteins >40 kD are prevented from entering tubular lumen by the glomerular filtration apparatus; thus, presence of high molecular weight proteins such as serum albumin in the urine is indicative of glomerular disease, whereas excretion of low molecular weight proteins suggests tubular absorption abnormalities.[11] SDS-PAGE analysis re-

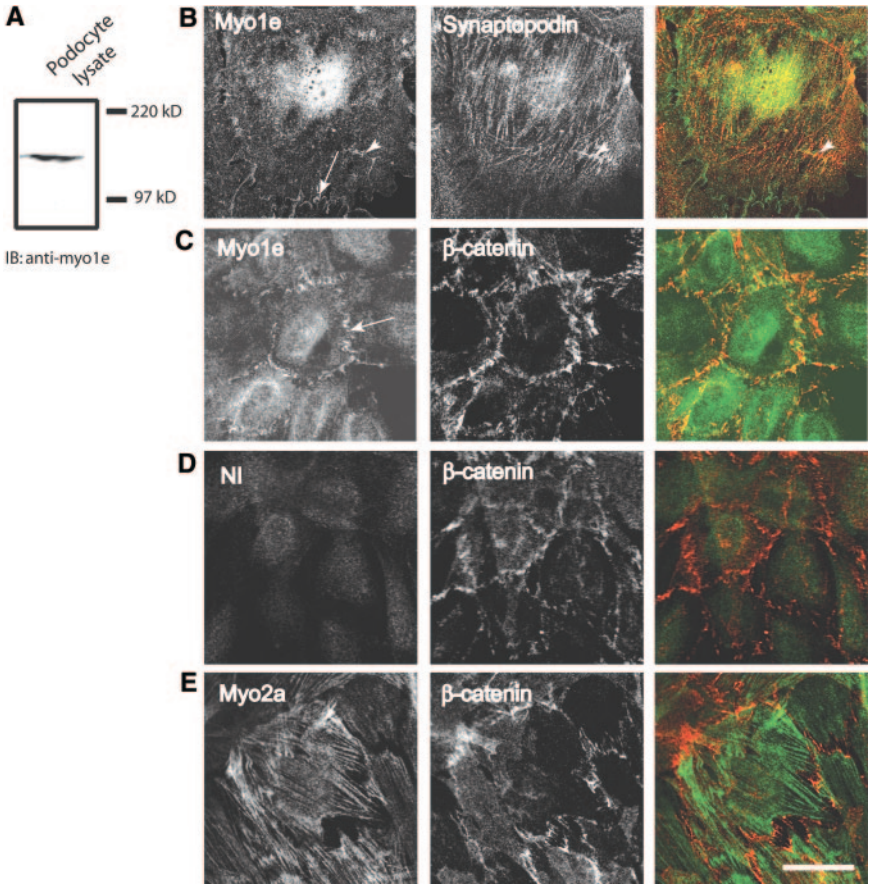

Figure 2. Myo1e is expressed in differentiated mouse podocytes. (A) Western blotting of podocyte lysate using anti-myo1e antibodies reveals the presence of a protein band corresponding to myo1e. (B through E) Immunofluorescence labeling of mouse podocytes using polyclonal antibodies against myo1e (B and C) and myo2a (E) as well as rabbit nonimmune (NI) antibodies (D). Myo1e localizes to punctate structures (arrowhead in B) and cell–cell junctions (arrows in B and C). Myo1e partially co-localizes with synaptopodin (B) and adherens junction marker β-catenin (C). NI antibody labeling (D) and labeling using Myo2a antibody (E) show lack of co-localization with the junctional marker. Bar = 20 μm. Merged images show polyclonal antibody labeling in green and mAb (anti-synaptopodin or anti–β-catenin) in red.

vealed that the major protein found in the urine of mutant mice was serum albumin (Figure 4A), indicating that the proteinuria was likely due to defects in the glomerular filtration barrier. This is consistent with the presence of blood/hemoglobin in the urine, which is also observed in some of the well-characterized glomerular diseases such as Alport syndrome as a result of the increased passage of red blood cells through the glomerular barrier.[12] The amount of albumin excreted by Myo1e-KO mice within a 24-h period was significantly higher than in their WT littermates ($P < 0.05$; Figure 4).

Visually, kidneys of Myo1e−/− mice appeared larger and paler than in their WT littermates (Figure 4C). In 8- to 12-wk-old mice, kidney/body weight ratio was significantly higher (approximately 1.5 -fold) in −/− mice than in their +/+ littermates ($P < 0.005$; Figure 4C).

To characterize the severity of renal impairment in Myo1e-KO mice, we measured levels of blood urea nitrogen (BUN) in the serum of WT and KO mice. BUN levels in WT mice were normal, and there was little variation in BUN levels among individual mice (Figure 4D). The average BUN level in KO mice was higher than in the WT mice ($P < 0.05$), and a wide range of BUN concentrations was observed among KO mice (Figure 4D, Table 1). These results indicate that renal function in the KO mice is compromised but the level of renal impairment varies among individual animals, an observation that is also confirmed by the variability in urinary albumin excretion level. Individual variability in the severity of renal impairment was also observed in the mouse model of Alport syndrome[13]; thus, such variability may be a common feature of glomerular disease in mouse genetic models.

Absence of Myo1e Leads to Defects in Glomerular Organization

Kidneys of Myo1e-KO mice exhibited signs of glomerular damage, including FSGS (glomeruli with thickened and closed capillary loops, partially obstructed by extracellular matrix [ECM]) and excessive ECM deposition in and around glomeruli (Figure 5, A through C; Table 1). Percentage of glomeruli that exhibited sclerosis in the KO mice was 7.5 ± 4.5 ($n = 3$). We also observed the presence of periodic acid-Schiff–positive casts in renal tubules as well as periodic acid-Schiff–positive protein resorption droplets in proximal tubules (Figure 6, Supplemental Figure 1). Both of these defects may result from proteinuria, because excretion of high levels of protein in the urinary filtrate promotes both formation of proteinaceous casts and enhanced protein degradation in proximal tubule cells. We also observed an increase in ECM deposition and cell infiltration in the juxtaglomerular and interstitial space, indicating the development of interstitial fibrosis, a common hallmark of renal injury (Figure 5).

Examination of glomerular proteins using immunofluorescence microscopy showed normal expression and localization of major glomerular markers, such as nephrin, podocin, and integrin α 3 in the KO mice (data not shown). To determine whether renal dysfunction observed in Myo1e-KO mice was related to immune mechanisms, such as autoimmune disease or immune complex deposits, we stained kidneys of WT and mutant mice with antibodies against IgA, IgG, and third component of complement (C3). No increase in the glomerular C3,

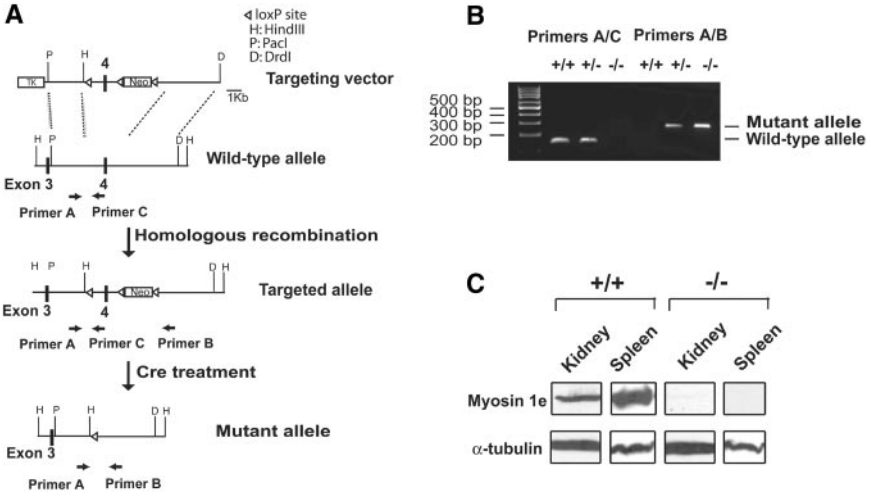

Figure 3. Generation and characterization of Myo1e-KO mice. (A) Gene targeting strategy and probes for genotyping. Homologous recombination between the gene targeting vector and the WT Myo1e allele was used to create a targeted allele of the Myo1e gene. The targeted allele contained insertion of the LoxP sites and Neomycin resistance gene, but the exon structure of the Myo1e gene remained intact. Cre-mediated recombination in mice carrying the targeted allele resulted in germline deletion of exon 4 of Myo1e gene and formation of a mutant (functionally null) allele. Primers A, B, and C were used for genotyping by genomic PCR, with primers A and C designed to amplify a 140-bp fragment from WT allele and with primers A and B designed to produce a 260-bp fragment from mutant allele. (B) Characterization of Myo1e-KO mice by genomic PCR. Genomic DNA samples isolated from WT mice (+/+), mice homozygous for Myo1e mutant allele (−/−), and heterozygous mice (+/−) were used as a template for PCR with primer pairs A/C and A/B. PCR with the primer pair A/C produced a 140-bp band only in mice that carried at least one copy of the WT allele, and PCR with the primer pair A/B resulted in a 260-bp band in mice that carried at least one copy of the mutant allele. (C) Western blotting of tissue samples from WT and Myo1e-KO mice. Spleen and kidney samples were probed using anti-myo1e antibody. Antibody against α-tubulin was used as a control for equal protein loading. No myo1e signal was detected in samples from the KO mice.

IgG, or IgA staining (Figure 5D and data not shown) and no electron-dense immune deposits (Figure 7) were observed in the glomeruli of mutant mice. Thus, immune dysfunction did not seem to contribute to the development of glomerular disease in Myo1e-KO mice. Conversely, immunofluorescence labeling revealed granular deposits of C3 and IgG in the proximal tubules of Myo1e-null mice (Figure 5D and data not shown). This is consistent with the published data indicating that in rodent models of proteinuria, exposure of proximal tubules to IgG and complement as a result of defective filtration leads to deposition of IgG and C3 in proximal tubules.[14] Complement deposited in the proximal tubules may then serve as a local proinflammatory signal that promotes tubular injury and infiltration of inflammatory cells. Next, we characterized renal changes in mutant mice using electron microscopy (EM). Whereas podocytes in the glomeruli of adult (2 to 4 mo old) WT mice formed numerous well-defined foot processes, in podocytes of myo1e-null mice, foot processes were effaced (flattened; Figure 7, Table 1). The average number of foot processes per unit length of the basement membrane was decreased 2.6-fold as a result of the flattening of foot processes. The average thickness of glomerular basement membrane (GBM) was increased nearly two-fold in Myo1e−/− mice, and the basement membrane organization was disrupted (Figure 7). Whereas GBM in WT mice showed typical three-layered organization, there were no easily identifiable layers in the GBM of mutant mice, and multiple electron-lucent areas were present within the GBM. Electron micrographs of proximal renal tubules in Myo1e−/− mice revealed signs of tubular injury, such as the loss of the apical brush border and presence of numerous electron-dense particles (either protein resorption droplets or lysosomes) in some tubules (Figure 6B).

Myo1e-KO Mice Develop Glomerular Filtration Defects within the First Month of Life

To determine whether defects in glomerular filtration and organization arose during early renal development or later in life, we examined urine and tissue samples from mice at the ages of 1 and 3 wk. Renal development in mice is completed by approximately 2 wk after birth; thus, the time points that we selected provide information about the state of the glomerular filtration apparatus both during kidney development and immediately after glomerular maturation is completed. At the age of 1 wk, urine of both WT and myo1e-KO mice contained a small amount of albumin (Figure 8A), possibly as a result of an incompletely developed and slightly leaky filtration barrier; the degree of proteinuria was comparable between the WT and KO mice. By 3 wk of age, WT mice exhibited no proteinuria, whereas myo1e-KO mice developed a high level of proteinuria (Figure 8A). Whereas glomerular filtration defects in myo1e-KO were not apparent at 1 wk of age, glomerular ultrastructure in the KO mice was abnormal even at this young age, with the average density of foot processes being significantly lower ($P \leq 0.001$), and the average GBM thickness being significantly higher than in the WT mice ($P \leq 0.05$; Figure 8B). By the age of 3 wk, foot process effacement and GBM thickening were even more pronounced ($P \leq 0.001$; Figure 8B). Overall, foot process architecture in younger KO mice (Figure 8) seemed somewhat more normal than in the 2-mo-old KO mice (Figure 7), indicating that glomerular architecture continues to deteriorate as the mice age. Slit diaphragms appeared normal in both 1- and 3-wk-old mice (Figure 8 and data not shown), indicating that glomerular

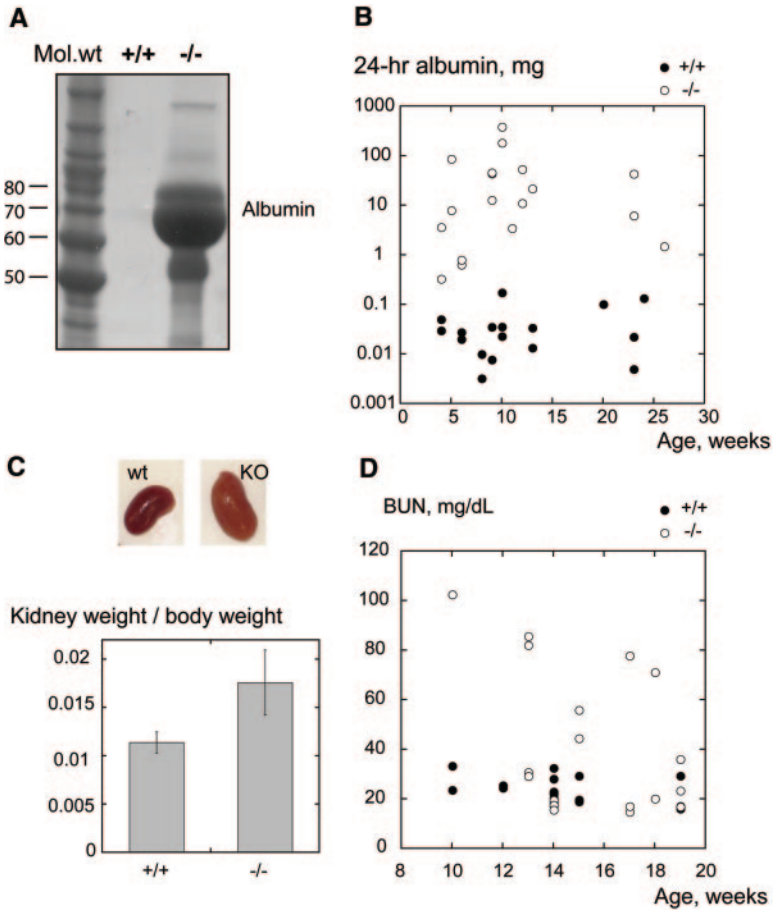

Figure 4. Myo1e-KO mice have impaired renal function. (A) Myo1e-null mice exhibited massive proteinuria. Urine samples (2 μl) from WT and KO mice were separated by SDS-PAGE, and proteins were stained using Coomassie Blue. The prominent protein band corresponds to serum albumin. (B) Absence of Myo1e leads to albuminuria. Albumin concentration in 24-h samples of urine collected from WT mice and KO mice at the ages of 4 to 32 wk was measured using ELISA with anti-mouse albumin antibodies. Each dot represents one mouse (*y* axis is shown in logarithmic scale). Average albumin concentration was significantly higher in KO mice ($P < 0.05$). (C) Increased kidney weight in Myo1e-KO mice. (Top) Representative photographs of WT and KO kidneys; the kidney of a KO mouse is larger and paler than the WT. (Bottom) Kidney weight to body weight ratio comparison. Kidney weight and body weight were measured in five WT and six KO mice aged 12 to 18 wk; average kidney weight to body weight ratio was higher in the KO mice ($P < 0.005$). Error bars represent SD. (D) Myo1e-KO mice have increased BUN levels. The level of BUN was measured in serum samples from WT and KO mice. Each dot represents one mouse.

filtration defects were not due to the absence of slit diaphragms.

DISCUSSION

Selective filtration in the glomerulus requires proper composition and organization of the GBM and formation of filtration slits between interdigitated podocyte foot processes. Podocytes are central to the establishment of glomerular filtration barrier because they are involved both in GBM secretion and filtration slit assembly. Most glomerular diseases are characterized by dramatic changes in podocyte structure and functions,[15] and many inherited glomerular diseases in humans have been attributed to mutations in podocyte-expressed proteins.[9,10]

In this study, we show that myo1e is expressed in podocytes and that KO of Myo1e gene in mice results in defects in renal filtration and podocyte organization. In the absence of myo1e, podocytes exhibit effacement of foot processes, a structural change that is typically observed in glomerular diseases and may represent either the cause of impaired filtration (as a result of the disruption of filtration slit architecture) or the consequence of defective filtration.[16] Glomeruli of Myo1e-KO mice also exhibit GBM thickening and disorganization, which is reminiscent of structural changes observed in some of the inherited renal diseases, such as Alport syndrome.[17,18] Analysis of renal function in Myo1e-KO mice revealed severe proteinuria as well as elevated BUN levels, both of which indicate impaired renal filtration. Although impaired glomerular filtration may also be caused by the deposition of antibodies or antibody–antigen complexes in the glomerulus, we did not observe immune complex deposits by EM. Thus, the observed renal defects do not seem to be immune mediated but rather result from impaired podocyte functions.

Defects in renal filtration in Myo1e-KO mice are not congenital but rather develop during the first weeks of life, possibly as the result of the increased hydrostatic pressure in the glomerulus after birth. Although filtration slit assembly seems to be normal, both foot processes and basement membrane exhibit defects early in the course of renal development, suggesting that foot process effacement, disruption of GBM assembly, or both events combined may be the cause of glomerular abnormalities in Myo1e-KO mice.

Kidneys of Myo1e-KO mice exhibited hallmarks of chronic renal injury, including tubulointerstitial fibrosis and glomerulosclerosis. In addition, some of the proximal tubules in the kidneys of Myo1e-null mice showed signs of excessive protein degradation and loss of the apical brush border. These changes in the proximal tubule organization are likely the consequence of the high protein concentration in the urinary filtrate, which results in enhanced protein absorption and degradation in the proximal tubule cells as well as the presence of complement and various serum-derived growth factors in the tubulointerstitial space. Release of complement and growth factors may then promote inflammation and fibrosis.[14]

The only study to date to investigate myo1e functions *in*

Table 1. Analysis of the renal phenotype in Myo1e-KO mice[a]

Abnormal Findings	WT	KO
Casts	1 of 6	6 of 6
Interstitial fibrosis	0 of 5	4 of 5
Glomerular ECM deposits by trichrome staining	0 of 4	3 of 4
EM: effacement	0 of 2	2 of 2
EM: GBM changes	0 of 2	2 of 2
BUN above 35 mg/dl	0 of 20	8 of 20

[a]The numbers indicate the number of animals analyzed and the number of animals that exhibited renal abnormalities.

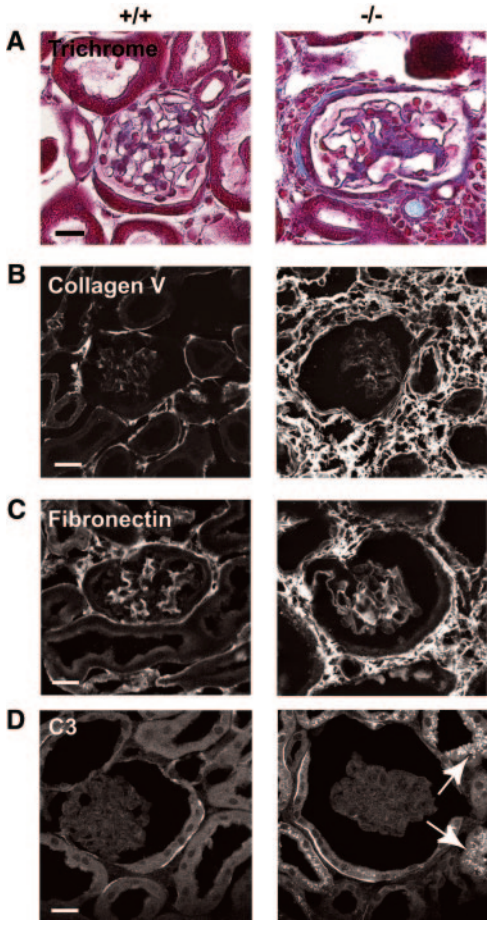

Figure 5. Myo1e-KO mice develop renal inflammation and fibrosis. (A through D) Paraffin-embedded sections (A) or frozen sections (B through D) or of mouse kidneys were stained using Trichrome stain to reveal extracellular matrix deposits (A) or using antibodies against collagen V (B) and fibronectin (C) or mouse C3 (D). (A) Trichrome staining of kidneys from Myo1e-KO mice revealed juxtaglomerular deposition of collagen (blue) and cell infiltration into the interstitial space. (B and C) Immunofluorescence staining indicated increased deposition of collagen V (B) and fibronectin (C) in the kidneys of KO mice. (D) Proximal tubules of Myo1e-KO mice contained granular deposits of C3 (arrows). Complement deposits were not observed in the kidneys of WT mice. Bars = 20 μm.

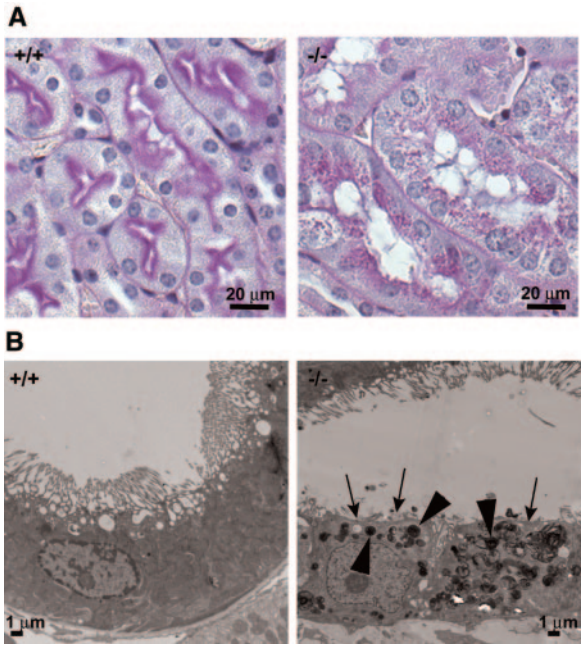

Figure 6. Proximal tubule changes in the kidneys of Myo1e-null mice. (A) Periodic acid-Schiff staining revealed numerous periodic acid-Schiff–positive granules in the proximal tubules of Myo1-null mice, indicating increased protein degradation. (B) Examination of kidney sections from WT and Myo1e-null mice using EM showed that some proximal tubules in the Myo1e-null mice exhibited loss of the apical brush border (arrows) and the presence of numerous inclusions that may represent lysosomes or protein resorption droplets (arrowheads).

vivo used a gene trap approach to disrupt Myo1e gene in mice.[19] This analysis was conducted as a part of a large effort to identify genes that act downstream of PDGF during pre- and postnatal development and to analyze the effects of disruption of PDGF target genes on mouse development. In this study, we inactivated Myo1e gene using homologous recombination in embryonic stem cells, an approach that resulted in the complete ablation of myo1e protein expression as confirmed by immunoblotting and immunofluorescence staining. Myo1e-KO mice described in our study exhibit significant renal impairment, whereas renal abnormalities were not detected in the gene-trap study.[19] Gene-trap construct insertion occurred in the first intron of Myo1e gene. The lack of protein expression in Myo1e gene-trap mutant mice has not been verified, and it is possible that gene-trap insertion produced a hypomorphic, rather than a null, allele. Because the first exon of Myo1e gene encodes only one amino acid, it is possible that initiation of transcription from another methionine (22 amino acids downstream of the first) or alternative splicing around the gene-trap insertion site could have resulted in synthesis of partially functional protein. In fact, residual protein expression in gene-trap mutants is a fairly common occurrence.[20] In addition, our observations show that whereas an increase

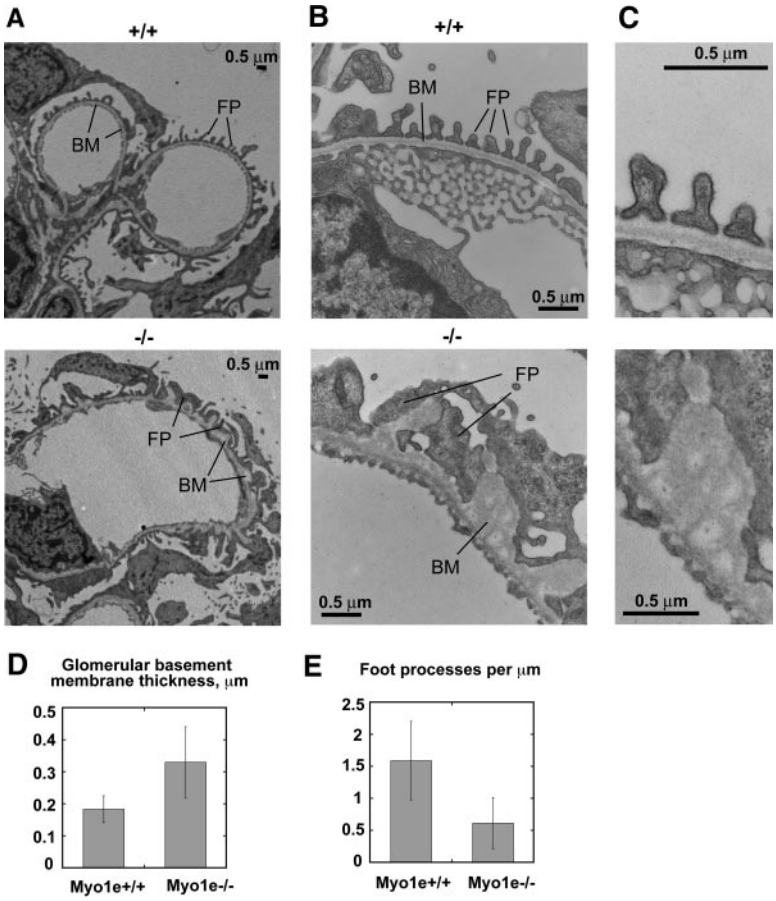

Figure 7. Characterization of the glomerular lesions in Myo1e-null mice by EM. (A and B) Low-magnification (A) and high-magnification (B) electron micrographs of glomeruli from 2-mo-old WT and KO mice. Myo1e-null mice exhibit thickening and disorganization of the basement membrane (BM) and effacement of podocyte foot processes (FP). (C) Additional magnification of the electron micrographs shown in B shows normal three-layered GBM organization in WT mice and disorganized GBM in the KO mice. (D and E) Quantitative analysis of the electron micrographs of renal sections collected from WT and KO mice. (D) Average thickness of GBM is increased in the KO mice. (E) Average number of foot processes per unit length of GBM is decreased in the KO mice. Error bars represent SD.

in urinary albumin excretion is readily observed in all Myo1e-null mice, BUN levels in Myo1e-null mice are highly variable, with some animals exhibiting normal BUN concentration. This result suggests a possibility that the tests used to characterize Myo1e gene–trapped mouse mutant (hematoxylin-eosin staining to evaluate overall renal morphology and BUN measurements to analyze renal functions) may have missed renal changes induced by Myo1e gene disruption.

Podocyte structural organization is guided by the actin cytoskeleton, which provides the driving force for foot process formation and support for junctional complex assembly.[21,22] Disruption of actin organization, as well as mutations or deletions of actin-binding proteins, leads to structural and functional defects in podocytes.[23,24] Our finding that myo1e plays an important role in podocyte functions further underscores the importance of the actin cytoskeleton for podocyte biology. Identification of an actin-dependent molecular motor as an important contributor to podocyte structure and functions adds a new player to the cast of molecular characters that already includes regulators of actin dynamics (Nck and synaptopodin), actin bundlers (α-actinin-4), and actin-binding scaffold proteins (ZO-1) (reviewed in reference 21). We previously determined that in addition to interacting with actin *via* its head (motor) domain, myo1e binds dynamin *via* its tail domain.[8] Recent experimental evidence showed that expression of dominant negative dynamin constructs caused actin reorganization and cell shape changes in podocytes and that proteolytic degradation of dynamin may be responsible for impaired podocyte function in some types of renal diseases.[25] It remains to be determined whether the effects of Myo1e KO on podocyte functions are mediated by changes in dynamin activity or result from a direct effect of myo1e on actin organization in podocytes. This will be the focus of future studies. In conclusion, our findings show that myo1e is expressed in podocytes and plays an important role in glomerular organization and functions.

CONCISE METHODS

Animal Studies

Animal experiments were approved by the Yale Institutional Animal Care and Use Committee. Mouse colonies were maintained in the Yale Animal Resources Center. Mouse urine was collected using metabolic cages and tested for protein, blood, and leukocytes using dipstick test strips. We conducted quantitative albumin measurements in 24-h urine samples using mouse albumin ELISA kit (Bethyl Labs, Montgomery, TX). We measured BUN levels using QuantiChrom Urea Assay Kit (BioAssay Systems, Hayward, CA).

Immunofluorescence Microscopy, Histochemistry, and EM

Mouse kidneys fixed by perfusion with periodate-lysine-paraformaldehyde fixative[26] were postfixed using periodate-lysine-paraformaldehyde (for cryosectioning) or 3.7% formaldehyde in PBS (for paraffin embedding). The list of antibodies used for immunofluorescence labeling and information on sectioning, immunostaining, image collection, and analysis is provided in Supplemental Methods.

Mouse kidneys were fixed for EM by perfusion with Karnovsky fixative (1.6% paraformaldehyde, 3% glutaraldehyde, and 0.5 mg/ml $CaCl_2$ in 0.1 M Na-cacodylate [pH 7.4]) and processed for EM as

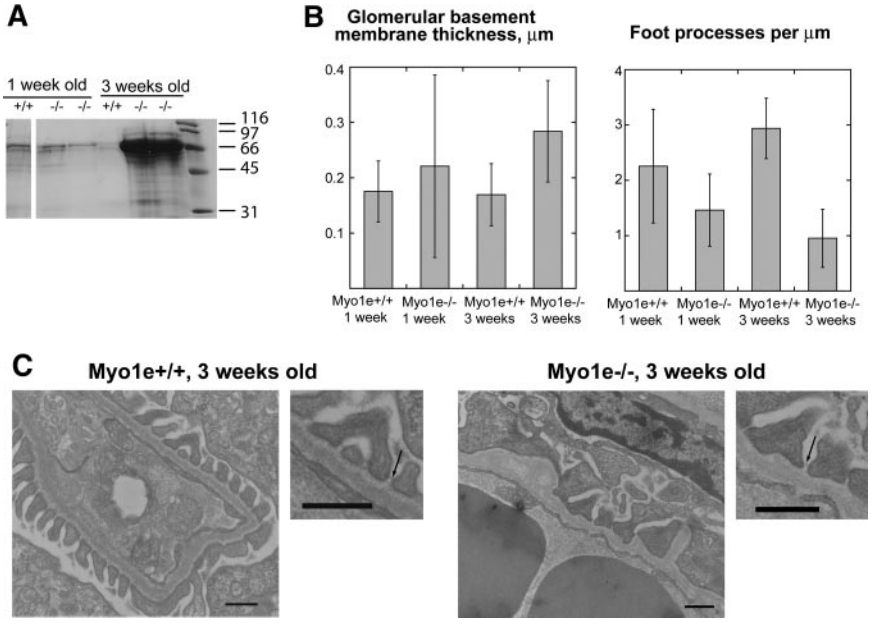

Figure 8. Characterization of glomerular defects during renal development in Myo1e-KO mice. (A) By the age of 3 wk, myo1e-null mice develop massive proteinuria. SDS-PAGE followed by Coomassie staining was used to analyze urine (1 μl of urine for each 3-wk-old KO mouse, 2 μl of urine for the other mice). (B) Morphometric analysis of glomerular ultrastructure shows an increase in GBM thickness and a decrease in foot process number in Myo1e-KO mice at the ages of 1 and 3 wk. Error bars represent SD. (C) Electron micrographs of glomeruli from 3-wk-old mice show normal foot process and GBM organization in WT mice and foot process effacement and GBM thickening in KO mice. Slit diaphragms (arrows) appear normal in both WT and KO. Bar = 0.5 μm.

described previously.[27] We collected images using a Jeol JEM-1230 electron microscope equipped with a digital camera.

Conditionally immortalized mouse podocytes were grown as described previously.[28] Differentiated podocytes were fixed using 3.7% formaldehyde in PBS, permeabilized using 0.2% Triton X-100 in PBS, and processed for indirect immunofluorescence.

SDS-PAGE and Immunoblotting

Urine samples were boiled with SDS sample buffer, separated using SDS-PAGE, and stained with Coomassie Brilliant Blue. To prepare tissue samples for immunoblotting, we homogenized cell or tissue samples in 5% TCA, washed them with cold water to remove TCA, and boiled then with SDS sample buffer. We performed SDS-PAGE and immunoblotting as described previously.[4]

ACKNOWLEDGMENTS

This work was supported by grants from the American Heart Association (0335441T) and American Diabetes Association (1-07-JF-39) to M. Krendel and from the National Institutes of Health (GM073823 and DK 25387) to M.S.M., DK 62289 to T.W., and HD32573 to M. Kashgarian. R.A.F. is an Investigator of the Howard Hughes Medical Institute.

We thank Peter Hegan, Sue Ann Mentone, Qingshang Yan, and Zhaopeng Du (Yale University) and Sharon Chase, Karen Maass, and Masako Nakatsugawa (SUNY UMU) for technical assistance; all members of Mooseker laboratory for valuable discussion and advice; and Drs. Joseph Madri (Yale University Medical School), Peter Mundel (University of Miami Miller School of Medicine), Lawrence Holzman (University of Michigan Medical School), and Michael DiPersio (Albany Medical College) for generously providing antibodies and cell lines.

DISCLOSURES

None.

REFERENCES

1. Foth BJ, Goedecke MC, Soldati D: New insights into myosin evolution and classification. *Proc Natl Acad Sci U S A* 103: 3681–3686, 2006
2. Krendel M, Mooseker MS: Myosins: Tails (and heads) of functional diversity. *Physiology (Bethesda)* 20: 239–251, 2005
3. Kim SV, Flavell RA: Myosin I: From yeast to human. *Cell Mol Life Sci* 65: 2128–2137, 2008
4. Tyska MJ, Mackey AT, Huang JD, Copeland NG, Jenkins NA, Mooseker MS: Myosin-1a is critical for normal brush border structure and composition. *Mol Biol Cell* 16: 2443–2457, 2005
5. Holt JR, Gillespie SK, Provance DW, Shah K, Shokat KM, Corey DP, Mercer JA, Gillespie PG: A chemical-genetic strategy implicates myosin-1c in adaptation by hair cells. *Cell* 108: 371–381, 2002
6. Kim SV, Mehal WZ, Dong X, Heinrich V, Pypaert M, Mellman I, Dembo M, Mooseker MS, Wu D, Flavell RA: Modulation of cell adhesion and motility in the immune system by Myo1f. *Science* 314: 136–139, 2006
7. Bement WM, Wirth JA, Mooseker MS: Cloning and mRNA expression of human unconventional myosin-IC: A homologue of amoeboid myosins-I with a single IQ motif and an SH3 domain. *J Mol Biol* 243: 356–363, 1994
8. Krendel M, Osterweil EK, Mooseker MS: Myosin 1E interacts with synaptojanin-1 and dynamin and is involved in endocytosis. *FEBS Lett* 581: 644–650, 2007
9. Kestila M, Lenkkeri U, Mannikko M, Lamerdin J, McCready P, Putaala H, Ruotsalainen V, Morita T, Nissinen M, Herva R, Kashtan CE, Peltonen L, Holmberg C, Olsen A, Tryggvason K: Positionally cloned gene for a novel glomerular protein—nephrin—is mutated in congenital nephrotic syndrome. *Mol Cell* 1: 575–582, 1998
10. Boute N, Gribouval O, Roselli S, Benessy F, Lee H, Fuchshuber A, Dahan K, Gubler MC, Niaudet P, Antignac C: NPHS2, encoding the glomerular protein podocin, is mutated in autosomal recessive steroid-resistant nephrotic syndrome. *Nat Genet* 24: 349–354, 2000
11. D'Amico G, Bazzi C: Pathophysiology of proteinuria. *Kidney Int* 63: 809–825, 2003
12. Kashtan CE: Familial hematuria due to type IV collagen mutations: Alport syndrome and thin basement membrane nephropathy. *Curr Opin Pediatr* 16: 177–181, 2004
13. Miner JH, Sanes JR: Molecular and functional defects in kidneys of mice lacking collagen alpha 3(IV): Implications for Alport syndrome. *J Cell Biol* 135: 1403–1413, 1996

14. Abbate M, Zoja C, Rottoli D, Corna D, Perico N, Bertani T, Remuzzi G: Antiproteinuric therapy while preventing the abnormal protein traffic in proximal tubule abrogates protein- and complement-dependent interstitial inflammation in experimental renal disease. *J Am Soc Nephrol* 10: 804–813, 1999
15. Wiggins RC: The spectrum of podocytopathies: A unifying view of glomerular diseases. *Kidney Int* 71: 1205–1214, 2007
16. Shankland SJ: The podocyte's response to injury: Role in proteinuria and glomerulosclerosis. *Kidney Int* 69: 2131–2147, 2006
17. Bernstein J: The glomerular basement membrane abnormality in Alport's syndrome. *Am J Kidney Dis* 10: 222–229, 1987
18. Rheault MN, Kren SM, Thielen BK, Mesa HA, Crosson JT, Thomas W, Sado Y, Kashtan CE, Segal Y: Mouse model of X-linked Alport syndrome. *J Am Soc Nephrol* 15: 1466–1474, 2004
19. Schmahl J, Raymond CS, Soriano P: PDGF signaling specificity is mediated through multiple immediate early genes. *Nat Genet* 39: 52–60, 2007
20. Voss AK, Thomas T, Gruss P: Efficiency assessment of the gene trap approach. *Dev Dyn* 212: 171–180, 1998
21. Faul C, Asanuma K, Yanagida-Asanuma E, Kim K, Mundel P: Actin up: Regulation of podocyte structure and function by components of the actin cytoskeleton. *Trends Cell Biol* 17: 428–437, 2007
22. Garg P, Verma R, Holzman LB: Slit diaphragm junctional complex and regulation of the cytoskeleton. *Nephron Exp Nephrol* 106: e67–e72, 2007
23. Yao J, Le TC, Kos CH, Henderson JM, Allen PG, Denker BM, Pollak MR: Alpha-actinin-4-mediated FSGS: An inherited kidney disease caused by an aggregated and rapidly degraded cytoskeletal protein. *PLoS Biol* 2: e167, 2004
24. Huber TB, Kwoh C, Wu H, Asanuma K, Godel M, Hartleben B, Blumer KJ, Miner JH, Mundel P, Shaw AS: Bigenic mouse models of focal segmental glomerulosclerosis involving pairwise interaction of CD2AP, Fyn, and synaptopodin. *J Clin Invest* 116: 1337–1345, 2006
25. Sever S, Altintas MM, Nankoe SR, Moller CC, Ko D, Wei C, Henderson J, Del Re EC, Hsing L, Erickson A, Cohen CD, Kretzler M, Kerjaschki D, Rudensky A, Nikolic B, Reiser J: Proteolytic processing of dynamin by cytoplasmic cathepsin L is a mechanism for proteinuric kidney disease. *J Clin Invest* 117: 2095–2104, 2007
26. McLean IW, Nakane PK: Periodate-lysine-paraformaldehyde fixative: A new fixation for immunoelectron microscopy. *J Histochem Cytochem* 22: 1077–1083, 1974
27. Thomson RB, Mentone S, Kim R, Earle K, Delpire E, Somlo S, Aronson PS: Histopathological analysis of renal cystic epithelia in the Pkd2WS25/- mouse model of ADPKD. *Am J Physiol Renal Physiol* 285: F870–F880, 2003
28. Mundel P, Heid HW, Mundel TM, Kruger M, Reiser J, Kriz W: Synaptopodin: An actin-associated protein in telencephalic dendrites and renal podocytes. *J Cell Biol* 139: 193–204, 1997

Supplemental information for this article is available online at http://www.jasn.org/.